4th IASPEI / IAEE International Symposium:

Effects of Surface Geology on Seismic Motion

August 23–26, 2011 · University of California Santa Barbara

PROPOSAL OF EXTENDED STORONG-MOTION ESTIMATION METHOD BASED ON SITE AMPLIFICATION AND PHASE CHARACTERISTICS FOR THE 2011 TOHOKU, JAPAN, EARTHQUAKE

Atsushi WAKAI
Port and Airport Research Institute
Japan

Atsushi NOZU
Port and Airport Research Institute
Japan

ABSTRACT

In this paper, an extended practical strong-motion estimation method is proposed for the 2011 off the Pacific coast of Tohoku, Japan, earthquake (M_{JMA}9.0). After a large earthquake, it is important to estimate strong ground motions at a site where engineering structures are damaged. Hata *et al.* [2011] proposed an efficient estimation method based on site amplification and phase characteristics, which does not require a fault model. The method cannot be directly applied, however, to a multiple-shock event such as the 2011 Tohoku earthquake. In order to circumvent this problem, the authors develop a new method in which the conventional method is applied to each subevent successively. Then, the method is applied to the 2011 Tohoku earthquake and its applicability is investigated.

INTRODUCTION

After a damaging earthquake, in order to clarify causes and mechanisms of the damage, it is important to estimate strong ground motions at the sites where there were damaged engineering structures.

The 2011 off the Pacific coast of Tohoku, Japan, earthquake caused significant damage to coastal structures, not only due to tsunamis but also due to strong ground motions [e.g., Takahashi *et al*., 2011]. There is an urgent need for the estimation of strong ground motions at sites of damaged structures that can be used for earthquake response analysis of structures and/or shake table tests.

As one of the methods to estimate strong ground motions from a large earthquake at a target site, a practical strong-motion estimation method was proposed by Hata *et al.* [2011]. The method is based on records of aftershocks both at the target site and at a nearby permanent strong-motion station, and on a record of the main shock at the strong-motion station. Because it focuses not only on the difference of site amplification factors but also on the difference of site phase characteristics between the target site and the strong-motion station, it can generate time histories of strong ground motions at the target site, which are required in the earthquake response analysis and/or shake table tests. Another great advantage of the method is its simplicity. Unlike full strong-motion simulations such as those based on the Stochastic Green's function method [Kowada *et al*., 1998], the method does not require a fault model of the large event. It is not necessarily easy to obtain an accurate fault model of a large event at an early stage of response to the large event. The method is expected to meet the needs of engineering community by providing a prompt estimation of strong ground motions.

The method, however, cannot be directly applied to a multiple-shock event such as the 2011 Tohoku earthquake, especially when contributions from two or more subevents are comparable for the target site. In this paper, an extended practical strong-motion estimation method is proposed for solving this problem. In this method, the conventional method is applied to each subevent successively. As an example, this extended method is applied to records at two closely-located permanent stations in Miyagi prefecture, Tohoku District, Japan, for the 2011 Tohoku earthquake. And then the validity of the estimation method is evaluated by comparing the estimated and observed strong ground motions at one of the permanent stations.

THE CONVENTIONAL AND PROPOSED METHOD

The conventional practical strong-motion estimation method [Hata *et al*., 2011] is simply composed of three steps. First, the Fourier amplitude of strong motion at a target site for a large earthquake is evaluated by correcting the Fourier amplitude at a nearby permanent strong-motion station for the same event based on the difference of the site amplification factors at the two sites. Then, the Fourier phase of strong motion at the target site for the large earthquake is approximated by the Fourier phase at the same site for a small earthquake that occurred close to the main rupture area of the large earthquake. Finally, an inverse Fourier transform is conducted to obtain the time histories of strong ground motions at the target site for the large earthquake.

One of the key assumptions of the method is that the Fourier phase for the large event is approximated by the Fourier phase for a small event, and, in fact, it has been shown that the assumption is appropriate for many of recent damaging earthquakes in Japan [e.g., Nozu, 2005; Nozu, 2007; Nozu and Irikura, 2008]. It is obvious, however, that the assumption cannot be directly applied to a multiple-shock event such as the 2011 Tohoku earthquake, especially when contributions from two or more subevents are comparable for the target site. In fact, contributions from at least two subevents are quite evident in the waveforms observed in Miyagi Prefecture, Japan, during the 2011 event as shown in the next section. Even in such cases, one could still expect that the Fourier phase corresponding to each subevent is approximated by the Fourier phase for a small event (this part will be confirmed later in this article).

Thus, the authors extend the conventional method and develop a new method that can be applied to records for a multiple-shock event. That is, first, a waveform at a permanent station is divided into parts corresponding to each subevent. Then, the conventional method is applied to each part, and waveforms at the target site corresponding to each subevent are obtained. In the end, waveforms are superposed to obtain the total waveform at the target site.

APPLICATION TO THE 2011 TOHOKU EARTHQUAKE

Outline of application

In this section, the proposed method is applied to the 2011 off the Pacific coast of Tohoku earthquake. The earthquake occurred on 11 March 2011 off the Pacific coast of Tohoku and Kanto district, Japan. According to the Japan Meteorological Agency (JMA) unified source catalog, the hypocentral parameters are origin time 14:46 (Japan Standard Time); epicenter, 38.1°N, 142.9° E; depth, 24 km; and JMA magnitude M_{JMA} 9.0. According to the F-net of the National Research Institute for Earth Science and Disaster Prevention, the moment magnitude is M_w 8.7.

Strong ground motions from the 2011 earthquake were observed in nationwide strong-motion networks in Japan including K-NET (Kinoshita, 1998), KiK-net (Aoi *et al.*, 2000), the network for Japanese ports (Nozu and Wakai, 2010), *etc.* In this section, we especially focus on two closely-located permanent strong-motion stations as shown Figure.1: Sendai-G in the strong-motion network for Japanese ports and MYG013 (K-NET Sendai), both of which successfully recorded the 2011 main shock. Figure.2 shows the observed velocity waveforms on the ground surface at Sendai-G and at MYG013. They are band-pass filtered between 0.2 and 2.0 Hz. Note that all of the velocity waveforms in this paper are band-pass filtered between 0.2 and 2 Hz. In Figure 2, contributions from at least two subevents are clearly found in the velocity waveforms. Peak ground velocity (PGV) for Sendai-G is 15.63(cm/s) and that for MYG013 is 80.48(cm/s). It is found that PGV for MYG013 is about five times as large as that for Sendai-G.

As an example, we assume that strong ground motions from the main shock at MYG013 are not obtained while strong ground motions from the main shock at Sendai-G are obtained. And then, strong ground motions at MYG013 are estimated from those at Sendai-G by means of the proposed method. By comparing the estimated and observed strong ground motions at MYG013, the applicability of the proposed method to a multiple-shock event such as the 2011 earthquake is investigated.

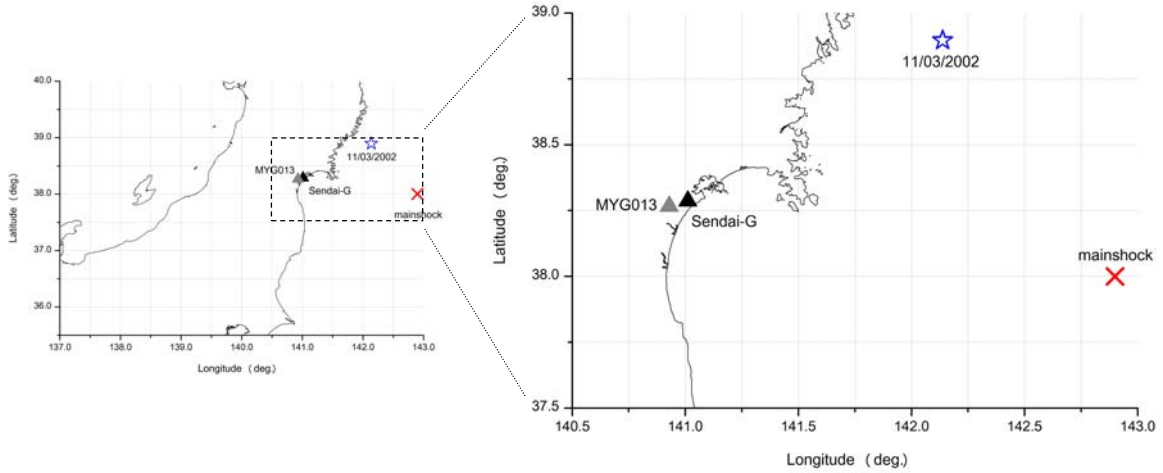

Fig. 1. The location of the two permanent strong-motion stations. Black and gray triangles respectively indicate Sendai-G and MYG013. The shortest distance between the stations is around 6.1km. A red cross and a blue star respectively indicate the epicenters of the main shock and the smaller event used to approximate the Fourier phase of the main shock in the following section.

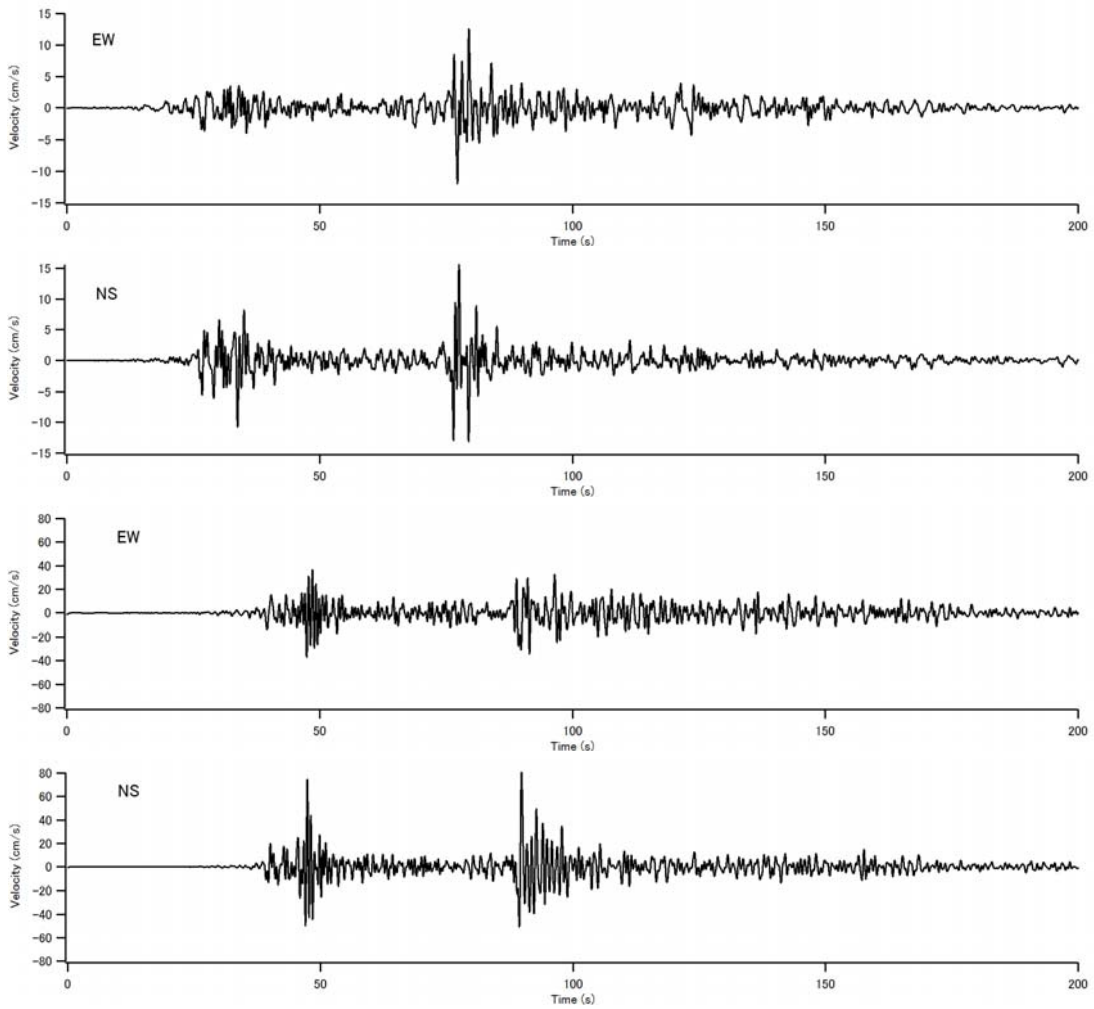

Fig. 2. Observed velocity waveforms at Sendai-G (upper two traces) and at MYG013 (lower two traces). All of the traces are band-pass filtered between 0.2 and 2 Hz. PGV at Sendai-G is 15.63(cm/s) ,that at MYG013 is 80.48(cm/s).

Removal of effect due to nonlinear behavior of local soft soil deposit at Sendai-G

A strong motion from a large event such as the 2011 earthquake often causes nonlinear behavior of local soft soil deposit. Thus, to begin with, we investigate nonlinear behavior of local soft soil deposit at Sendai-G, taking the advantage of the fact that borehole records are also available at Sendai-G. Figure 3 shows the surface-to-borehole Fourier spectral ratios at Sendai-G for the main shock and for some past smaller earthquakes for which the soil behaved linearly. Fourier spectra are the root mean square of the two horizontal components. All of the spectra are smoothed with a Parzen window with a bandwidth of 0.05 Hz. All of the spectral ratios have peaks at around 8.0 Hz, except for the main shock, for which the peak is slightly shifted to a lower frequency. At the same time, the peak level of the spectral ratio for the main shock is lower than those for the smaller earthquakes. This indicates a slight nonlinear behavior of the local soft soil deposit at Sendai-G for the main shock. Therefore, in order to remove the effect due to the nonlinear behavior, nonlinear and linear multiple reflection theory is repeatedly applied to the records of the main shock at Sendai-G.

First, nonlinear and linear ground models are created for Sendai-G. Starting from a ground model based on PS logging, S-wave velocities and damping factors are tuned so that the theoretical surface-to-borehole spectral ratios become consistent with the observed ones (Figure 3). The results are shown in Table 1 and Table 2. As shown in Figure 4, the nonlinear and linear spectral ratios can almost be reproduced by using these ground models.

Next, multiple reflection method is applied to the record of the main shock on the ground surface at Sendai-G by using the ground model shown in Table 1 and then the strong motion on the firm ground outcrop is obtained. Then, multiple reflection method is applied to the strong motion on the firm ground outcrop by using the ground model shown in Table 2 to obtain a strong motion on the ground surface at Sendai-G without the effect of soil nonlinearity. In Figure 5, the linear and nonlinear (observed) velocity waveforms are compared. Black traces are for the linear case and gray, dashed traces are for the nonlinear case. The difference of the waveforms is small, indicating that the effect of soil nonlinearity on the velocity waveforms was marginal.

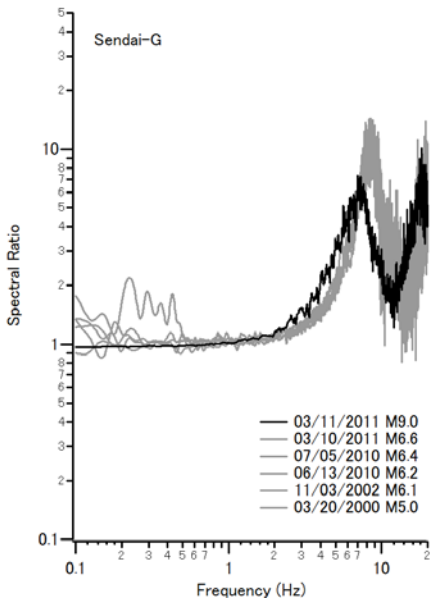

Fig.3. Fourier spectral ratios (Surface/GL-10.4m) at the vertical array station at Sendai-G. Fourier spectra are the root mean square of the two horizontal components. All of the spectra are smoothed with a Parzen window with a bandwidth of 0.05 Hz.

Table 1. Nonlinear ground model at Sendai-G

Thickness of layer (m)	Vs (m/s)	Density (g/cm^3)	Damping factor
3.0	149.5	1.75	0.09
4.0	207.0	1.85	0.09
3.4	820.0	2.40	0.09
-	820.0	2.40	-

Table 2. Linear ground model at Sendai-G

Thickness of layer (m)	Vs (m/s)	Density (g/cm^3)	Damping factor
3.0	182.0	1.75	0.05
4.0	252.0	1.85	0.05
3.4	820.0	2.40	0.05
-	820.0	2.40	-

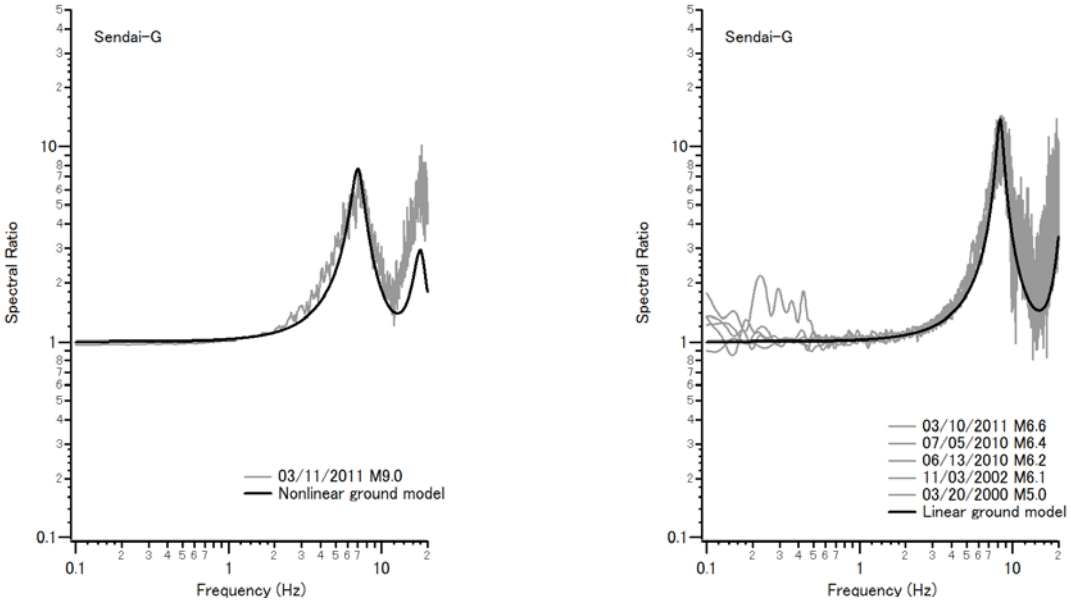

Fig.4. Comparison of theoretical and observed surface-to-borehole spectral ratios. The left side is for the nonlinear case, and the right side is for the linear case.

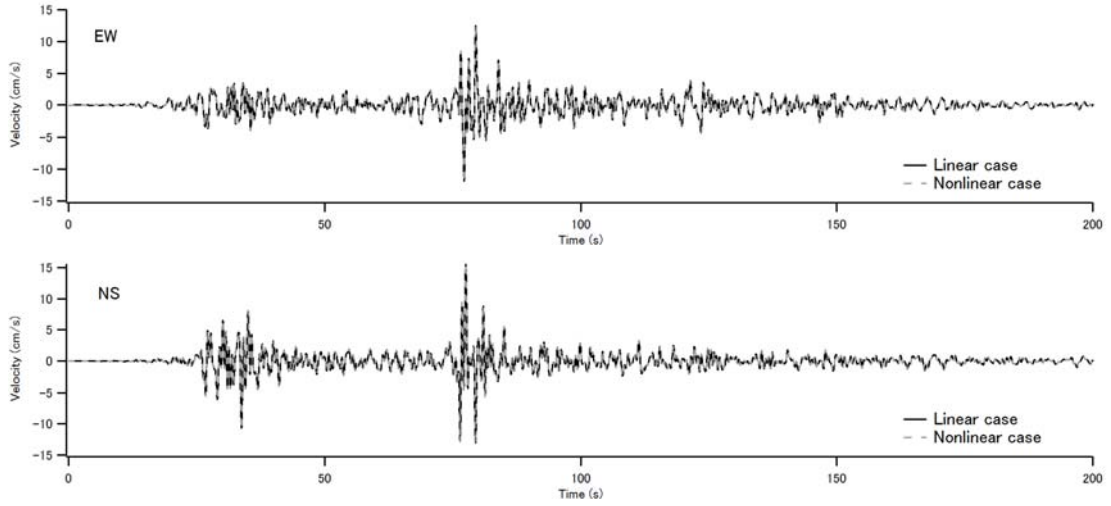

Fig.5. Nonlinear and linear velocity waveforms on the ground surface at Sendai-G. Black traces are for the linear case and gray, dashed traces are for the nonlinear case. All of the waveforms are band-pass filtered between 0.2 and 2.0Hz. For both components, the waveforms are almost the same.

Division of the waveforms at MYG013 into parts

The linear waveforms shown in Figure 5 are tapered off between 45 and 65 s to obtain the former and the latter parts as shown in Figures 6 and 7, each corresponding to different subevents.

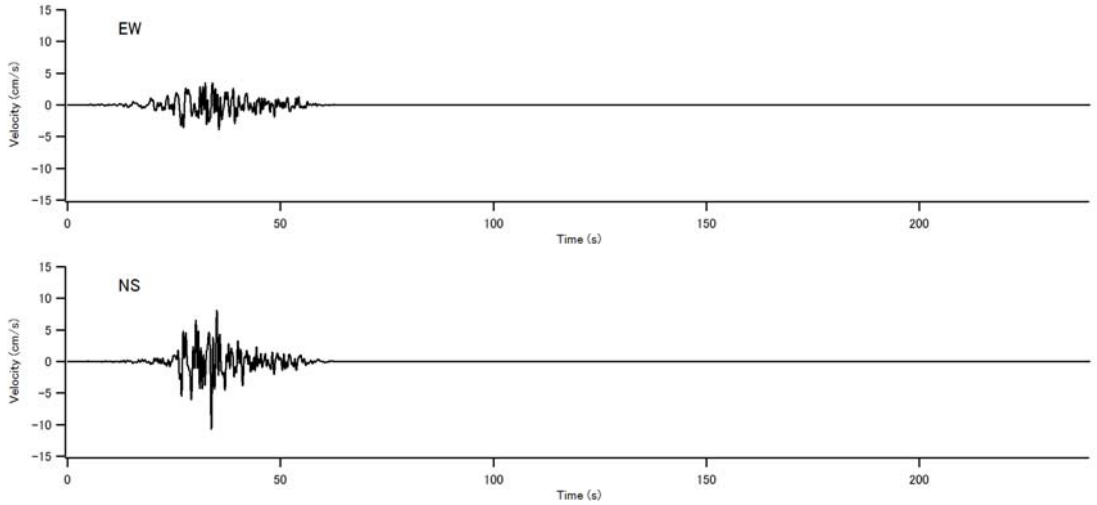

Fig. 6. The former parts of linear velocity waveforms on the ground surface at Sendai-G.

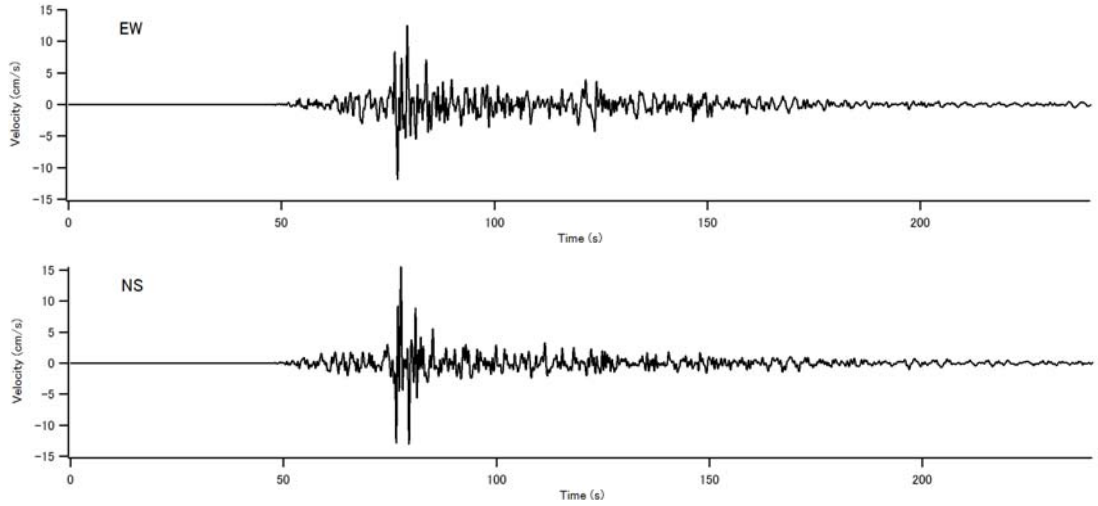

Fig. 7. The latter parts of linear velocity waveforms on the ground surface at Sendai-G.

Estimation of Fourier amplitude

The Site amplification factors at Sendai-G and at MYG013 are shown in Figure 8 [Nozu and Nagao, 2005]. It can be recognized that the site amplification factors are quite different for these sites although the two sites are relatively close. The Fourier amplitudes for MYG013 are estimated as follows: First, for the former parts of the linear waveforms at Sendai-G, Fourier amplitude spectra are calculated and multiplied by the ratio of the site amplification factors at MYG013 and Sendai-G (MYG013/Sendai-G) to obtain Fourier amplitude spectra on the ground surface at MYG013 corresponding to the former parts based on the following equations.

[EW component at MYG013] = [EW component at Sendai-G] *[ratio of site amplification factors; MYG013/Sendai-G] (1)

[NS component at MYG013] = [NS component at Sendai-G] *[ratio of site amplification factors; MYG013/Sendai-G] (2)

The same procedure is applied to the latter parts of the linear waveforms at Sendai-G to obtain Fourier amplitude spectra on the ground surface at MYG013 corresponding to the latter parts.

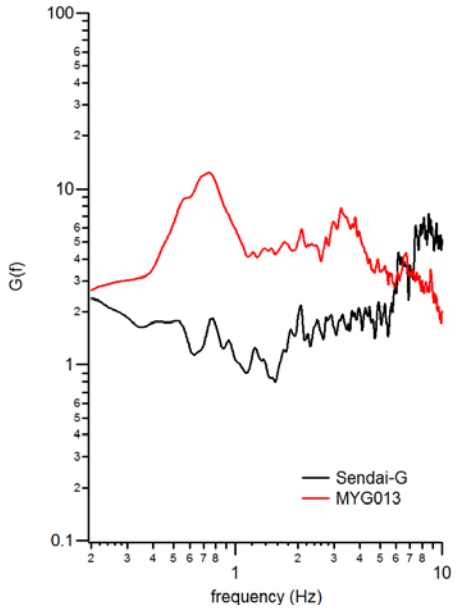

Fig. 8. Site specific amplification factors at Sendai-G and at MYG013. Black trace is for Sendai-G and red trace is for MYG013. Site amplification factors are quite different for the two stations.

Estimation of Fourier phase

According to Hata *et al*. [2011], it is desirable to select a small event that is close to the main rupture area of the main shock. In the present case, a smaller event shown in Table 3 was selected both for the former parts and for the latter parts, referring to its relative location to the main shock. Validity of this selection can be confirmed as follows. In Figure 9, the observed velocity waveforms for the main shock on the ground surface at Sendai-G are shown as black traces, both for the former and the latter parts. On the other hand, the red traces indicate the synthetic velocity waveforms with the Fourier amplitude of the main shock and the Fourier phase of the smaller event on the ground surface at Sendai-G. The upper two are for the former parts, and the lower two are for the latter parts. In Figure 9, we can recognize the similarity of the synthetic waveforms to the observed ones, especially for the latter parts. The similarity of the waveforms indicates that the record of the main shock and that of the smaller event have almost the same Fourier phase; that is, although the 2011 event is a multiple-shock event, the Fourier phase for the former and the latter parts of the main shock waveforms can still be approximated by the Fourier phase of the smaller event. Thus, the Fourier phase of the smaller event at MYG013 is used in the following strong-motion estimation.

Table 3. Parameters for the smaller event used to approximate the Fourier phase of the main shock. Parameters for the main shock are also represented.

Date (mm/dd/yyyy)	Time (hh:mm JST)	Latitude (deg.)	Longitude (deg.)	Depth (km)	M_{JMA}
*03/11/2011	14:46	38.100N	142.900E	24	9.0
11/03/2002	12:37	38.896N	142.138E	46	6.1

* The main shock

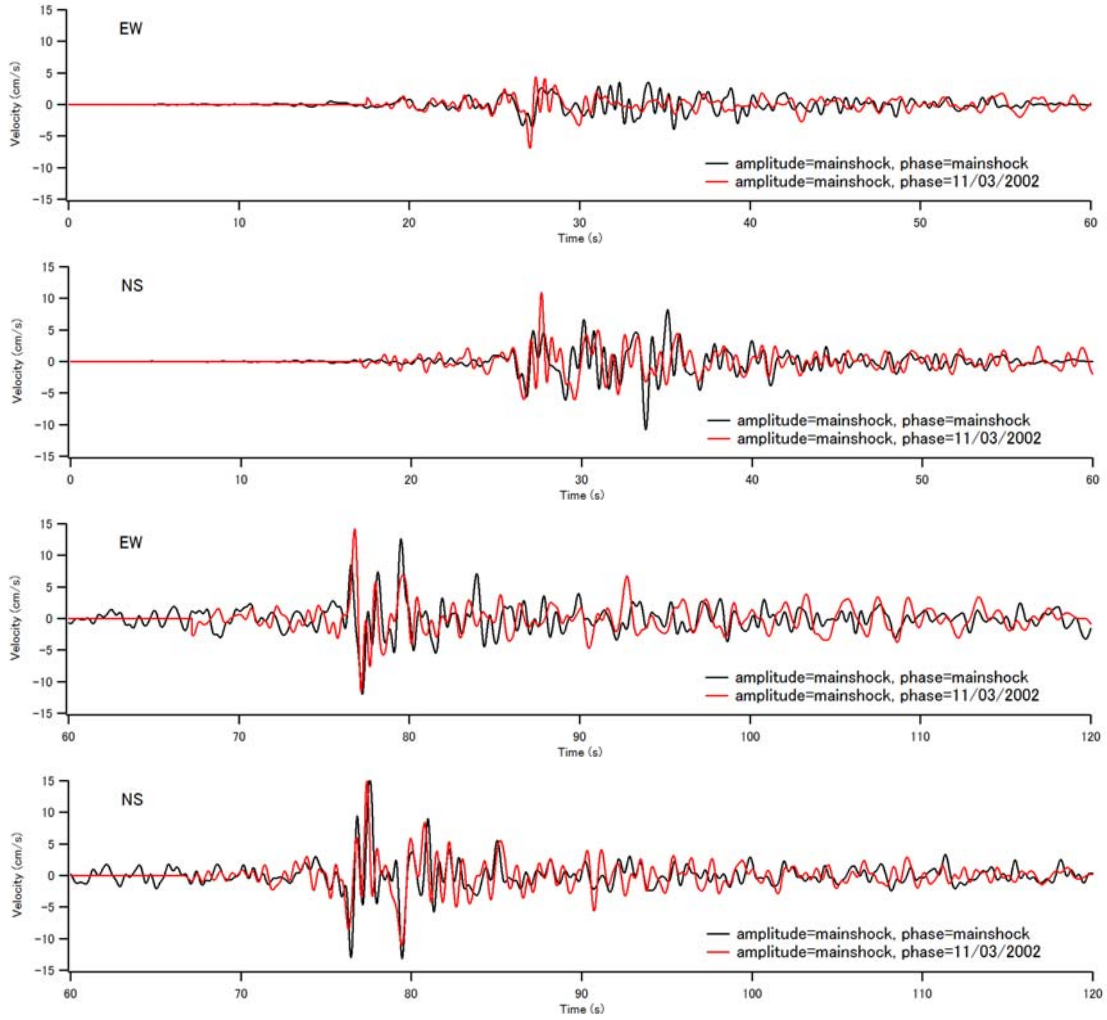

Fig. 9. The observed velocity waveforms for the main shock on the ground surface at Sendai-G (black traces) and the synthetic velocity waveforms with the Fourier amplitude of the main shock and the Fourier phase of the 11/03/2002 event (red traces) on the ground surface at Sendai-G. The upper two are for the former parts and the lower two are for the latter parts. The velocity waveforms are band-pass filtered between 0.2 and 2 Hz. The similarity of the traces indicates that the Fourier phase of the main shock both for the former and the latter parts can be approximated by that of the 11/03/2002 event.

Estimation of strong motion

For the former and the latter parts of waveforms, strong motions on the ground surface at MYG013 are respectively estimated by making use of the Fourier amplitude and the Fourier phase estimated above. Finally, by superposing the former parts and the latter parts, strong motions from the main shock on the ground surface at MYG013 are estimated. In the superposition, the relative arrival time of the S waves at Sendai-G is considered. Note that in these estimations soil nonlinearity is not considered. In Figure 10, the estimated velocity waveforms (red traces) on the surface at MYG013 are compared with the observed ones (black traces). The velocity waveforms are band-pass filtered between 0.2 and 2 Hz. On the whole, strong motions from the main shock are reproduced fairly well. In Figure 11, the estimated Fourier amplitude spectrum for the main shock at MYG013 (red trace) is compared with the observed one (black trace). In Figure 11, the observed Fourier amplitude spectrum for the main shock at Sendai-G is also plotted for comparison (gray trace). Fourier spectra are the root mean square of the two horizontal components. The spectra are smoothed with a Parzen window with a bandwidth of 0.05 Hz. The estimated Fourier amplitude spectrum is quite similar to the observed one at MYG013, except for the overestimation of high frequencies probably due to the negligence of soil nonlinearity.

Thus, it is suggested that the proposed method is applicable to a multiple-shock event such as the 2011 Tohoku earthquake, for which

contributions from at least two subevents are evident. From an engineering point of view, it is quite important that a strong motion at a site without the record of the main shock can be estimated based on the record of the main shock at a nearby site even when the site effects are quite different for the two sites.

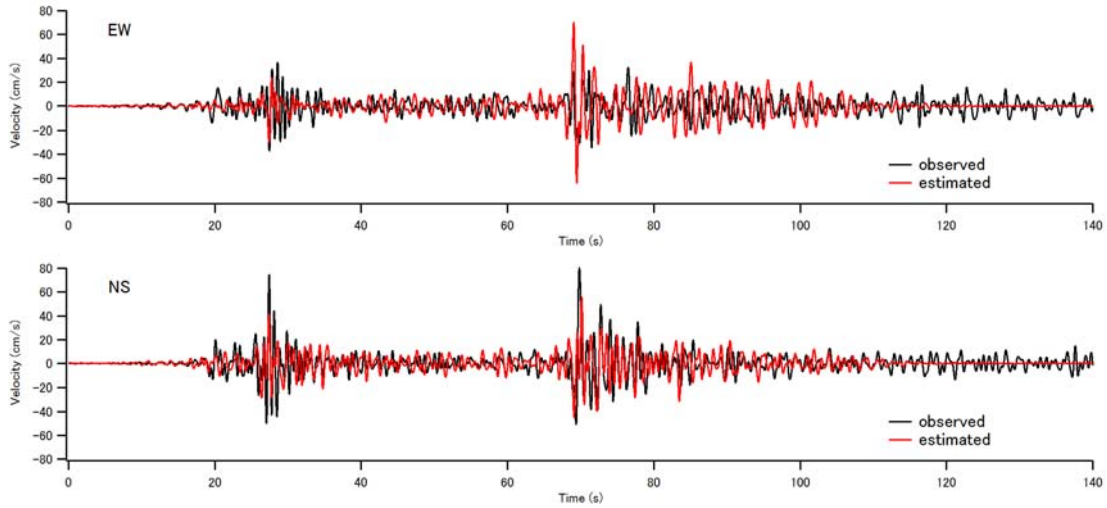

Fig. 10. The observed velocity waveforms (black traces) and the estimated velocity waveforms (red traces) on the ground surface at MYG013. The velocity waveforms are band-pass filtered between 0.2 and 2 Hz. The similarity of the traces indicates the applicability of the proposed method.

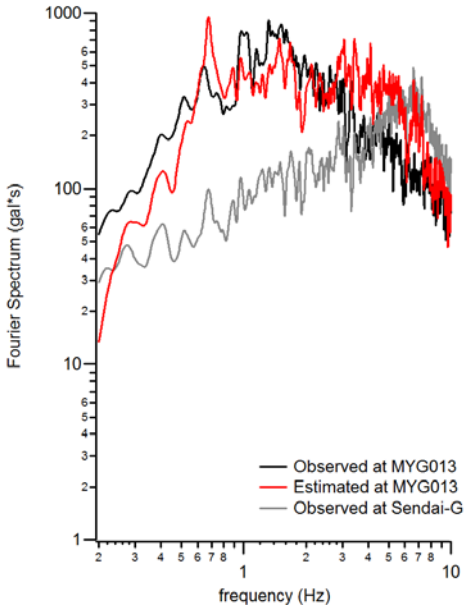

Fig. 11. The observed Fourier amplitude spectrum (black trace) and the estimated one (red trace) for the main shock on the ground surface at MYG013. Also plotted is the observed Fourier amplitude spectrum (gray trace) for the main shock on the ground surface at Sendai-G. The Fourier spectra are the root mean square of the two horizontal components. The spectra are smoothed with a Parzen window with a bandwidth of 0.05 Hz. The similarity of the traces at MYG013 indicates the applicability of the proposed method.

CONCLUSIONS

After a damaging earthquake such as the 2011 off the Pacific coast of Tohoku, Japan, earthquake, there is an urgent need for the estimation of strong ground motions at sites of damaged structures that can be used for earthquake response analysis of structures and/or shake table tests. Although the strong-motion estimation method proposed by Hata *et al.* [2011], which approximates the Fourier phase of the main shock at the target site with those of a smaller event, is advantageous because of its simplicity, it cannot be directly applied to a multiple-shock event such as the 2011 event, especially when contributions from two or more subevents are comparable for the target site. In this article, the authors extend the conventional method and develop a new method that can be applied to records for a multiple-shock event. In the new method, the waveform at the permanent station is divided into parts corresponding to each subevent and the conventional method is applied to each part. The proposed method is applied to the 2011 Tohoku earthquake to confirm its applicability. From the viewpoint of velocity waveforms and Fourier amplitude spectra, the estimated strong motion mostly reproduces the observed one at the target site. Thus, it is suggested that the proposed method is applicable, on the whole, to multiple-shock events such as the 2011 Tohoku earthquake.

ACKNOWLEDGEMENT

We would like to express our gratitude to the National Research Institute for Earth Science and Disaster Prevention (NIED), Japan, for providing important strong-motion data from K-NET. Also we would like to thank the Japan Meteorological Agency (JMA) for providing source parameters for the 2011 off the Pacific coast of Tohoku main shock and smaller events which happened before the 2011 main event.

REFERENCES

Aoi, S., K. Obara, S. Hori, K. Kasahara, and Y. Okada (2000), “New strong-motion observation network: KiK-net”, Eos Trans. Am. Geophys. Union, 81, p.329.

Hata, Y., A. Nozu, and K. Ichii [2011], “A practical method to estimate strong ground motions after an earthquake, based on site amplification and phase characteristics”, Bull. Seism. Soc. Am., Vol. 101, No. 2, pp. 688-700.

Kinoshita, S. (1998), “Kyoshin Net (K-net)”, Seim. Res. Lett., Vol. 69, No.4, pp.309-332.

Kowada, A., M. Tai, Y. Iwasaki, and K. Irikura [1998], “Evaluation of horizontal and vertical strong ground motions using empirical site-specific amplification and phase characteristics”, J. Struct. Constr. Eng., AIJ, No. 514, pp. 97-104 (in Japanese with English abstract).

Nozu, A. [2005], “Variable-slip rupture model for the 2004 Niigata-ken Chuetsu earthquake - waveform inversion with empirical Green's functions –“, Jour. Seism. Soc. Japan, Vol.58, No.3, pp.329-343 (in Japanese with English abstract).

Nozu, A. [2007], “Variable-slip rupture model for the 2005 West Off Fukuoka Prefecture earthquake - waveform inversion with empirical Green's functions –“, J. Seism. Soc. Japan, Vol.59, No.3, pp.253-270 (in Japanese with English abstract).

Nozu, A. and K. Irikura [2008], “Strong-motion generation areas of a great subduction-zone earthquake: waveform inversion with empirical Green's functions for the 2003 Tokachi-oki earthquake”, Bull. Seism. Soc. Am., Vol.98, No.1, pp.180-197.

Nozu, A. and A. Wakai [2010], “Annual report on strong-motion earthquake records in Japanese ports (2009)”, Technical Note of the Port and Airport Research Institute, No.1223 (in Japanese with English abstract).

Nozu, A. and T. Nagao [2005], “Site amplification factors for strong-motion sites in Japan based on spectral inversion technique”, Technical Note of the Port and Airport Research Institute, No. 1112 (in Japanese with English abstract).

Takahashi, S. *et al*. [2011], “Urgent Survey for 2011 Great East Japan Earthquake and Tsunami Disaster in Ports and Coasts”, Technical Note of the Port and Airport Research Institute, No. 1231, pp. 111-156 (in Japanese with English abstract).